

## Experimental Phase Synchronization of a Chaotic Convective Flow

D. Maza, A. Vallone, H. Mancini, and S. Boccaletti

*Department of Physics and Applied Mathematics, Universidad de Navarra, Irunlarrea s/n, 31080 Pamplona, Spain*  
(Received 22 December 1999; revised manuscript received 26 May 2000)

We report experimental evidence of phase synchronization of high dimensional chaotic oscillators in a laboratory experiment. The experiment consists of a thermocapillary driven convective cell in a time dependent chaotic regime. The synchronized states emerge as a consequence of a localized temperature perturbation to the heater. The transition to phase synchronization is studied as a function of the external perturbations. The existence and stability conditions for this phenomenon are discussed.

PACS numbers: 47.52.+j, 05.45.Xt, 05.45.Jn

In the last decade, synchronization of chaos has become a field of great interest. So far, four types of synchronization have been studied in the case of a coupling between two chaotic concentrated systems, namely, complete synchronization [1], generalized synchronization [2], phase [3], and lag synchronization [4]. Complete synchronization implies a perfect linking of the two chaotic trajectories, so as they remain in step with each other in the course of the time. Generalized synchronization implies the hooking of the output of one system to a given function of the output of the other system [2]. Phase synchronization (PS) refers to a process whereby two weakly coupled systems are characterized by a perfect locking of the chaotic phases, whereas the corresponding chaotic amplitudes remain uncorrelated. Finally, lag synchronization consists of the fact that the two signals become identical but shifted in time of a lag time [4].

Since its theoretical proposal [3], PS has been discovered to be ubiquitous in nature. Its emergence represents a key feature in the dynamics, e.g., of the human cardiorespiratory system [5], of an extended ecological system [6], of the magnetoencephalographic activity of Parkinsonian patients [7], and of the electrosensitive cells of the paddlefish [8].

In spite of a large body of evidence of PS in nature, the study of such a phenomenon in a controlled laboratory experiment is not yet available. In this Letter, we report experimental evidence of PS in a Bénard-Marangoni convective experiment. This kind of experimental system can be, in fact, considered a good candidate to approach the study of PS, due to the presence of two basic mechanisms ruling the chaotic behavior in the convective regime. Namely, the two mechanisms are the destabilization of the thermal boundary layer, creating isolated structures known as *thermals* or *thermal plumes*, and the large scale convective circulation of the main flow, dragging and scattering the *thermals* along the system [9–12].

Both mechanisms are present in the experimental setup presented in Fig. 1. A rectangular cell made by insulating material (Plexiglas) confines a layer of 100 cSt silicon oil (depth  $17.5 \pm 0.01$  mm, Prandtl number 937), whose surface is in contact with the atmosphere. The longitudinal

and transversal dimensions of the cell are 70 and 30 mm, respectively, thus determining a longitudinal (transverse) aspect ratio of  $70/17.5 = 4$  ( $30/17.5 \approx 1.71$ ). The fluid is inhomogeneously heated from below by an aluminum heater (dimensions  $40 \times 40$  mm) located at one extreme of the bottom of the cell, attached to one of the cell's wall. The heater temperature (monitored in the heater mass center) is kept constant at  $52 \pm 0.05$  °C by a proportional integrating-differentiating loop supplying an average power of 4.37 W. Under these conditions, the dynamics can be described by means of two main modes, namely, a bulk mode (a large cell-filling roll) and a boundary mode done by small scale thermal plumes originating close to the boundary layer. The bulk mode is preferentially excited by the asymmetric heating, while the boundary

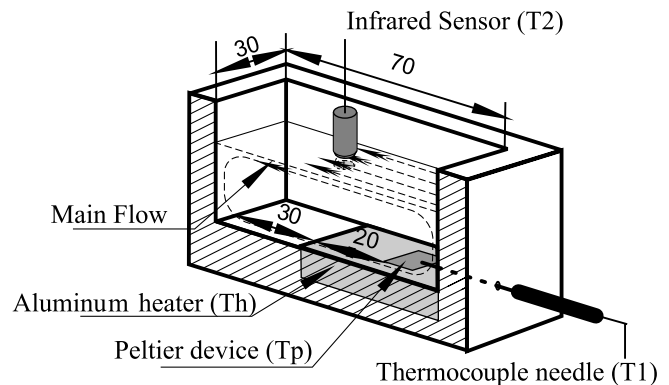


FIG. 1. The experimental setup. A rectangular cell made of Plexiglas confines a layer of 100 cSt silicon oil (depth  $17.5 \pm 0.01$  mm, Prandtl number 937). The longitudinal and transversal dimensions of the cell are 70 and 30 mm, respectively. The fluid is inhomogeneously heated from below by an aluminum heater located at one extreme of the bottom of the cell, attached to one of the cell's wall. Measurements are performed within the thermal boundary layer by a sensor  $T_1$  (a thermocouple needle located 15 mm from the cell's wall and 0.5 mm from the bottom) and on the surface of the flow by an infrared sensor  $T_2$ , integrating over an area of  $3 \text{ mm}^2$ . A thermoelectrical device (a Peltier cell of  $12 \times 12 \text{ mm}^2$ ) is inserted within the heater, driven by an external power. The streamlines depict the direction of the convective flow. Thermal plumes are drawn on the thermal boundary layer by the main flow.

mode is excited close to the cell bottom. The boundary (bulk) mode is associated with a high (low) frequency  $f_H = 4.46 \times 10^{-2}$  Hz ( $f_L = 9.39 \times 10^{-3}$  Hz) [11]. The two modes interact because the thermals originated at the boundary layer are dragged along the flow by the bulk mode and eventually reinjected into the boundary layer. We should point out that the reinjection mechanism of the thermals into the boundary layer is a peculiar property of the free surface boundary condition. In a Rayleigh-Bénard configuration, the existence of two boundary layers would produce either hot and cold thermals, which would interact throughout the transport phenomena determined by the mean flow [13]. A theoretical model for describing the effects of such an interaction in the above experimental setup has been recently offered [14], in terms of a delayed dynamical equation, through which the formation and propagation of space-time structures, such as phase defects, have been identified and controlled [15].

In order to characterize the dynamics, we measure the temperature oscillations within the thermal boundary layer by a sensor  $T_1$  (a thermocouple needle) and on the surface of the quasibidimensional flow by an infrared sensor  $T_2$ , integrating over an area of  $3 \text{ mm}^2$ , which corresponds approximately to that of the thermals dragged along the flow [14]. The two arising signals are chaotic, with an associated wide band power spectrum dominated by two main frequencies and their nonlinear combinations. However, the spectrum of the signal  $T_1$  is dominated by the frequency  $f_H$  because the corresponding measurement is performed within the boundary layer, and therefore it is only slightly affected by the contribution of the bulk mode. On the contrary, the spectrum of signal  $T_2$  shows  $f_L$  as principal frequency because, even though the corresponding measurement is sensitive to both modes, it is extracted from an area where plumes are less prevalent.

In order to produce phase synchronization between  $T_1$  and  $T_2$ , we have inserted a thermoelectrical device (a Peltier cell of  $12 \times 12 \text{ mm}^2$  area and 3 mm depth) within the heater, delivering a modulation of the temperature, controlled by a sinusoidal power  $W_p = A \sin(\omega t)$ . Such a modulation represents a tiny perturbation to the heater temperature (in the whole experiment, the effective energy dissipated in the Peltier cell has been less than 5% of the total energy dissipated in the heater). The external driving technique for the synchronization of chaotic oscillators has been theoretically proposed quite recently [16]. Within the experimental resolution (typically  $\pm 1.5 \times 10^{-5}$ ) the two frequencies  $f_H$  and  $f_L$  maintain an incommensurate ratio in the whole range of external perturbations. Let us discuss the meaning of phase synchronizing the signals  $T_1$  and  $T_2$ . The two modes of the dynamics are originated by very different physics mechanisms (a bulk spatially coherent convection and a boundary layer instability). Adjusting the phases of the measured signals implies adjusting the phase relationship with which the plumes are reinjected into the boundary layer by the main convective flow, that

is, determining a dynamical relationship between the two interacting modes. In the following, we will extract conditions for building up such phase relationships with the help of only a local small time dependent perturbation in the boundary layer.

In order to analyze the phases of the chaotic signals  $T_1$  and  $T_2$ , we have assumed the formalism proposed by Gabor [17], consisting of extracting the phase of a scalar signal  $s(t)$  from the associated complex analytic signal  $S(t) \equiv s(t) + i\tilde{s}(t)$ ;  $\tilde{s}(t) = \frac{1}{\pi} \text{PV} \int_{-\infty}^{\infty} \frac{s(\tau)}{t-\tau} d\tau$ , PV meaning that the integral is considered in the sense of the Cauchy principal value. From now on we will denote with  $\varphi_1$  ( $\varphi_2$ ) the phase extracted from the signal  $T_1$  ( $T_2$ ) and with  $\varphi_p$  the phase imposed by the sinusoidal modulation on the Peltier ( $\varphi_p \equiv \omega t$ ). The results are reported in Figs. 2 and 3.

Without forcing, the signals  $T_1$  and  $T_2$  are reported in Figs. 2a and 2b, respectively, together with their spectra (Figs. 2c and 2d). The two phases  $\varphi_1$  and  $\varphi_2$  evolve in an unsynchronized manner (Fig. 3a, region I). We then fix the amplitude of the perturbation at  $A = 1.85 \times 10^{-1}$  W, and gradually change  $\omega$ . By selecting  $\omega = 2\pi f_H$  (region II of Fig. 3a), the phase  $\varphi_1$  synchronizes with  $\varphi_p$ , while the perturbation does not affect the behavior of  $\varphi_2$ . The resulting signals are reported in Figs. 2e and 2f with the corresponding spectra in Figs. 2g and 2h. This fact suggests that forcing with the natural frequency of the boundary mode only the mechanism of thermal formation can be affected in the phase, while the bulk mode is essentially unaffected by the perturbation. In region III of Fig. 3a,  $\omega = 2\pi f_L$ . In this case, the perturbation is resonant with the frequency of the bulk mode, and therefore the phase  $\varphi_2$  synchronizes with  $\varphi_p$ , while  $\varphi_1$  evolves unsynchronized. Again, the corresponding signals (spectra) are reported in Figs. 2i and 2j (Figs. 2k and 2l). In order to obtain phase synchronization between bulk and boundary modes, one must select  $\omega$  to be the subharmonic of  $f_H$  close to  $f_L$ . In region IV of Fig. 3a,  $\omega = 2\pi f_S$  ( $f_S = 7.50 \times 10^{-3}$  Hz  $\approx \frac{f_H}{6}$ ). In this case, the perturbation succeeds in synchronizing the phases of the two signals. The signals  $T_1$  and  $T_2$  and their spectra are shown in Figs. 2m and 2n and Figs. 2o and 2p, respectively. A similar condition for the frequency of the control modulation was experimentally derived in another context, such as the control and suppression of the chaotic oscillations of a loss-modulated CO<sub>2</sub> laser [18]. A relevant difference here is that the signals remain chaotic in the collective PS state, that is, the perturbation does not change the chaotic high dimensional nature of the dynamics, but only determines the hooking of the phases of the chaotic signals. From Figs. 2m and 2n, one can see that the locking in the chaotic phases is not associated with any apparent correlation in the global chaotic signals. As for the high dimensionality of the chaotic signals  $T_1$  and  $T_2$ , by calculating in our data the *false nearest neighbors* dimension (FNND) [19], we have checked that, in all cases, the FNND came out to be 5 or greater. This fact

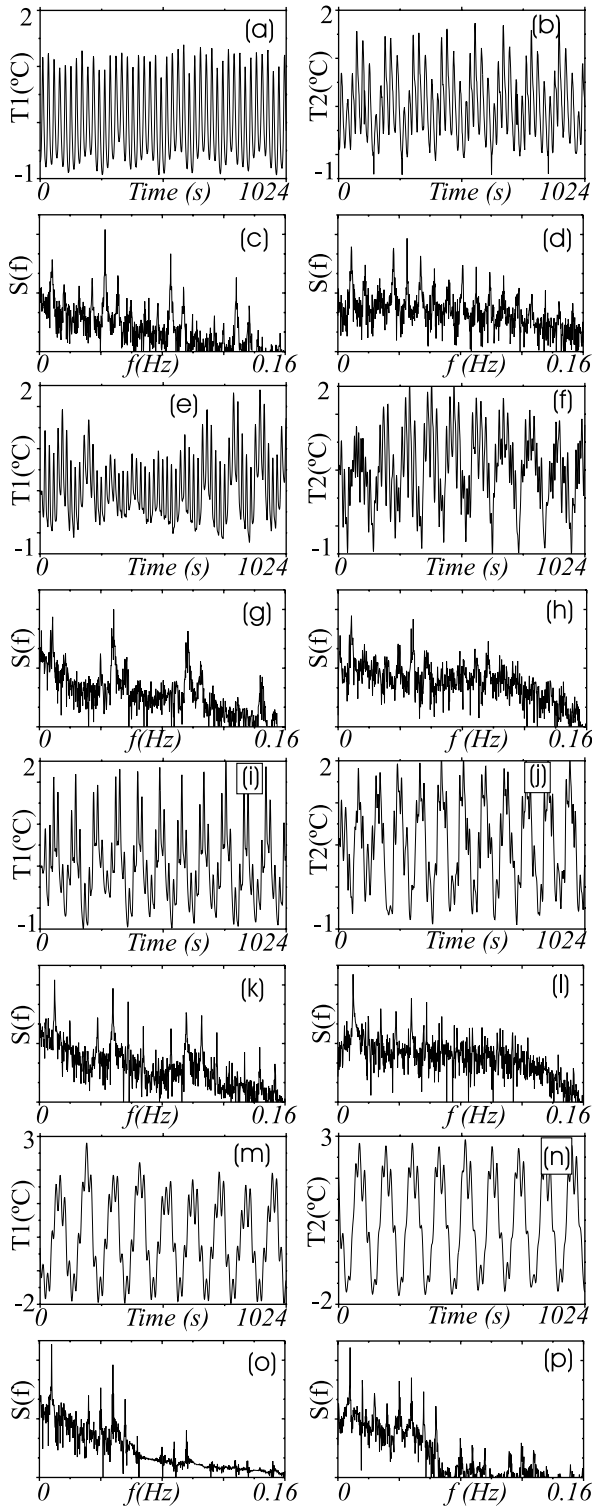


FIG. 2. Temporal behavior [(a),(b),(e),(f),(i),(j),(m),(n)] and Fourier spectra [(c),(d),(g),(h),(k),(l),(o),(p)] of the two signals  $T_1$  (left column) and  $T_2$  (right column). (a)–(d) Without forcing. (e)–(h)  $A = 1.85 \times 10^{-1}$  W,  $\varphi_p = 2\pi f_H t$ . (i)–(l)  $A = 1.85 \times 10^{-1}$  W,  $\varphi_p = 2\pi f_L t$ . (m)–(p)  $A = 1.85 \times 10^{-1}$  W,  $\varphi_p = 2\pi f_S t$ .

represents a noticeable difference with respect to phase locking phenomena studied in Rayleigh-Bénard configurations in the past [20], where the resulting dynamics consisted in a quasiperiodic state with commensurate ratio between the high and low frequencies associated to the boundary and bulk modes. Furthermore, phase locking has been observed in more recent experiments in self-sustained oscillations of a confined jet [21], in the pulsed dynamics of a fountain [22], in memory-induced low frequency oscillations in closed convection boxes [13], and in the coupling of rotating water jets by surface waves [23]. Again, the novelty in our experiment is the occurrence of phase synchronization phenomena within a chaotic regime induced by an external perturbation.

Let us now move to discuss how PS depends on the amplitude of the perturbation, at a given frequency. By setting  $\omega = 2\pi f_S$ , and gradually increasing  $A$ , we report in Fig. 3b the temporal behavior of  $\Delta\varphi_{2,p} \equiv |\varphi_2 - \varphi_p|$ . The figure clearly depicts the transition from the non-synchronized state ( $A = 0.035$  W) toward the phase synchronized state ( $A = 0.185$  W) through an intermediate state ( $A = 0.144$  W) where the system is at the borderline of phase synchronization, displaying  $2n\pi$  phase jumps

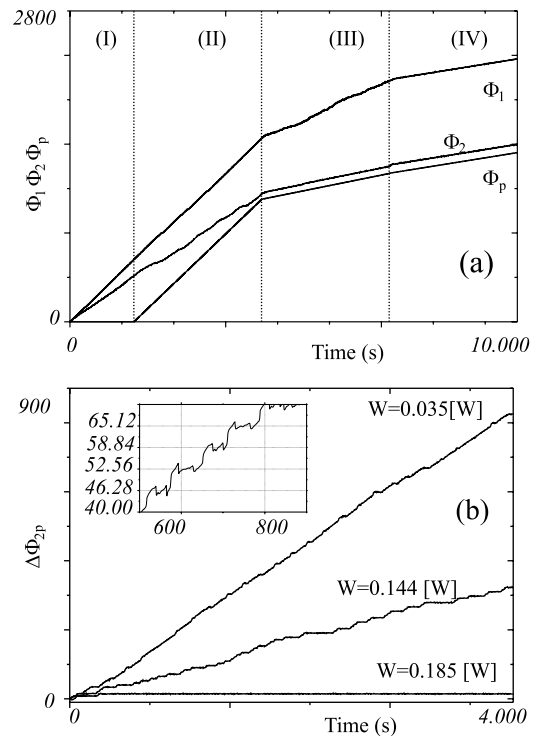


FIG. 3. (a) Temporal evolution of the phases  $\varphi_1$ ,  $\varphi_2$ , and  $\varphi_p$ . (Region I) Without forcing. (Region II)  $A = 1.85 \times 10^{-1}$  W,  $\varphi_p = 2\pi f_H t$ . (Region III)  $A = 1.85 \times 10^{-1}$  W,  $\varphi_p = 2\pi f_L t$ . (Region IV)  $A = 1.85 \times 10^{-1}$  W,  $\varphi_p = 2\pi f_S t$ . (b)  $\Delta\varphi_{2,p} \equiv |\varphi_2 - \varphi_p|$  (in radians) vs time (in seconds) for (I)  $A = 0.035$  W, (II)  $A = 0.144$  W, and (III)  $A = 0.185$  W. The inset zooms in on the echelon structure composed of the phase jumps occurring in (II).

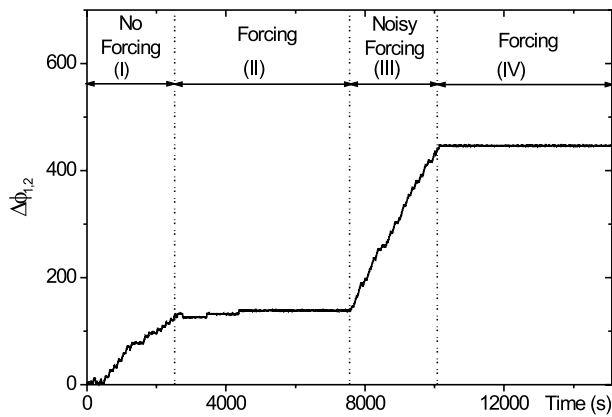


FIG. 4.  $\Delta\varphi_{1,2} \equiv |\varphi_1 - \varphi_2|$  (in radians) vs time (in seconds) without modulation (region I), with modulation ( $\omega = 2\pi f_S$ ,  $A = 0.185$  W, region II), with a noisy forcing (region III), and switching on again the sinusoidal modulation after noise (region IV).

( $n$  integer) among successive plateaus of constant phase difference (visible in the inset of the same figure). This intermediate state was theoretically predicted as a clear signature of the occurrence of phase synchronization [3].

Finally, we study the stability of PS in our experiment. In Fig. 4 we report the temporal behavior of  $\Delta\varphi_{1,2} \equiv |\varphi_1 - \varphi_2|$  during a long experimental trial in which we initially let the system evolve unperturbed (region I). The Peltier modulation was switched on at  $t = 2500$  s ( $\omega = 2\pi f_S$ ,  $A = 0.185$  W) to build up the phase synchronized state (region II). At time  $t = 7500$ , the driving modulation is changed to a random modulation. At each second we have updated the modulation power from a white noise flat distribution between 0 and 0.185 W. As a consequence, the system leaves the synchronized state (region III). Finally, at  $t = 10000$  s, the noisy modulation is rechanged into the previous sinusoidal modulation. The relevant result is that a phase synchronized state is again set in (region IV), thus demonstrating the stability of the collective state against external noise. Furthermore, looking at the two phase synchronized states (regions II and IV), one can appreciate the different transient time needed to reach synchronization. In particular, the noise is actually enhancing the occurrence of phase synchronization. The noise effect in enhancing PS will be reported in detail elsewhere.

The authors are indebted to Juergen Kurths for many fruitful discussions. Work was supported by Ministerio de Educación y Ciencia PB98-0208 (Spain),

PIUNA-University of Navarra and European Union. S.B. acknowledges financial support from EU Contract No. ERBFMBICT983466.

- [1] L. M. Pecora and T.L. Carroll, Phys. Rev. Lett. **64**, 821 (1990).
- [2] N. F. Rulkov, M. M. Sushchik, L. S. Tsimring, and H. D. I. Abarbanel, Phys. Rev. E **51**, 980 (1995); L. Kocarev and U. Parlitz, Phys. Rev. Lett. **76**, 1816 (1996).
- [3] M. G. Rosenblum, A. S. Pikovsky, and J. Kurths, Phys. Rev. Lett. **76**, 1804 (1996).
- [4] M. G. Rosenblum, A. S. Pikovsky, and J. Kurths, Phys. Rev. Lett. **78**, 4193 (1997).
- [5] C. Schafer, M. G. Rosenblum, J. Kurths, and H. H. Abel, Nature (London) **392**, 239 (1998).
- [6] B. Blasius, A. Huppert, and L. Stone, Nature (London) **399**, 354 (1999).
- [7] P. Tass, M. G. Rosenblum, J. Weule, J. Kurths, A. Pikovsky, J. Volkman, A. Schnitzler, and H.-J. Freund, Phys. Rev. Lett. **81**, 3291 (1998).
- [8] A. Neiman, X. Pei, D. Russell, W. Wojtenek, L. Wilkens, F. Moss, H. A. Braun, M. T. Huber, and K. Voigt, Phys. Rev. Lett. **82**, 660 (1999).
- [9] B. I. Shraiman and E. D. Siggia, Phys. Rev. A **42**, 3650 (1990).
- [10] J. Werne, Phys. Rev. E **48**, 1020 (1993).
- [11] H. Mancini and D. Maza, Phys. Rev. E **55**, 2757 (1997).
- [12] G. Zocchi, E. Moses, and A. Libchaber, Physica (Amsterdam) **166A**, 387 (1990).
- [13] E. Villermaux, Phys. Rev. Lett. **75**, 4618 (1995).
- [14] D. Maza, Ph.D. thesis, Universidad de Navarra, Spain, 1995.
- [15] S. Boccaletti, D. Maza, H. Mancini, R. Genesio, and F. T. Arecchi, Phys. Rev. Lett. **79**, 5246 (1997).
- [16] A. S. Pikovsky, M. G. Rosenblum, G. V. Osipov, and J. Kurths, Physica (Amsterdam) **104D**, 219 (1997).
- [17] D. Gabor, J. IEEE London **93**, 429 (1946).
- [18] A. N. Pisarchik, V. N. Chizhevsky, R. Corbalán, and R. Vilaseca, Phys. Rev. E **55**, 2455 (1997).
- [19] M. B. Kennel, R. Brown, and H. D. I. Abarbanel, Phys. Rev. A **45**, 3403 (1992).
- [20] J. P. Gollub and S. V. Benson, J. Fluid Mech. **100**, 449 (1980); M. Dubois and P. Bergé, J. Phys. (Paris) **42**, 167 (1981).
- [21] E. Villermaux and E. J. Hopfinger, Physica (Amsterdam) **72D**, 230 (1994).
- [22] E. Villermaux, Nature (London) **371**, 24 (1994).
- [23] F. Giorgiutti, L. Laurent, and F. Daviaud, Phys. Rev. E **58**, 512 (1998).